Heat Transfer Engineering, 27(4):53–63, 2006

ISSN: 0145-7632 print / 1521-0537 online
DOI: 10.1080/01457630500523816

Taylor & Francis
Taylor & Francis Group

Two-Phase Microfluidics for Semiconductor Circuits and Fuel Cells

CARLOS H. HIDROVO, THERESA A. KRAMER, EVELYN N. WANG, SÉBASTIEN VIGNERON, JULIE E. STEINBRENNER, JAE-MO KOO, FU-MIN WANG, DAVID W. FOGG, ROGER D. FLYNN, EON SOO LEE, CHING-HSIANG CHENG, THOMAS W. KENNY, JOHN K. EATON, and KENNETH E. GOODSON

Mechanical Engineering Department, Stanford University, Stanford, California, USA

Industrial trends are presenting major challenges and opportunities for research on two-phase flows in microchannels. Semiconductor companies are developing 3D circuits for which multilevel microfluidic cooling is important. Gas delivery microchannels are promising for PEM fuel cells in portable electronics. However, data and modeling are needed for flow regime stability, liquid entrainment/clogging, and bubble inception/departure in complex 2D and 3D geometries. This paper provides an overview of the Stanford two-phase microfluidics program, with a focus on recent experimental and theoretical progress. Microfabrication technologies are used to distribute heaters, thermometers, pressure sensors, and liquid injection ports along the flow path. Liquid PIV quantifies forces on bubbles, and fluorescence imaging detects flow shapes and liquid volume fraction. Separated flow models account for conjugate conduction, liquid injection, evaporation, and a variety of flow regimes. This work benefits strongly from interactions with semiconductor and fuel cell companies seeking validated models for product design.

INTRODUCTION

Over the past few decades and with the refinement of microfabrication techniques, the use of microchannels has become promising for a variety of industrial applications. Examples include biological applications for front end sample preparation (purification, separation, and concentration), cell sorting, and even more fundamental studies of mechanotransduction. Microchannels continue to play an integral part in thermal management (microchip cooling, microreactors) and energy systems (fuel cells, microcombustion) applications.

The authors would like to thank our sponsors, Honda R&D Co. Ltd., Intel Corporation, and DARPA, through their 3DIC intiative, not only for their support but also for their input, feedback, and insight.

Work was performed in part at the Stanford Nanofabrication Facility (a member of the National Nanofabrication Users' Network), which is supported by the National Science Foundation under grant ECS-9731293, its lab members, and the industrial members of the Stanford Center for Integrated Systems.

Address correspondence to Dr. Carlos H. Hidrovo, Building 530, Room 224, Mechanical Engineering Department, Stanford University, Stanford, CA 94305-3030. E-mail: hidrovo@stanford.edu

The effective use of microchannels in these applications requires a proper understanding of the physics underlying flow at these scales. Among the specifics is the behavior of multiphase flows at reduced dimensions. Liquid-vapor flows are of particular interest, as surface tension becomes so dominant at the microscale that macroscopic behavior no longer applies. A critical enabling tool in the understanding of the behavior of any type of flow is visualization, and much progress has been made recently using a variety of techniques based on high-resolution microscopy, fluorescence techniques, and micro PIV.

In addition, relatively straightforward experimental tasks, such as localized pressure and temperature measurements, become quite challenging at the microscale. In order to obtain locally distributed measurements, temperature and pressure sensors must be developed and integrated within the microchannel fabrication.

Two-phase flow in microchannels has received much attention, including a number of outstanding review articles in prior editions of the present microchannel conference. A generalized search on the topic returns thousands of relevant manuscripts. There are conferences specialized on the topic of fluid flow

in micro- and minichannels, and two-phase flow constitutes a leading topic [1]. Of particular interest has been the study of two-phase flow in microchannels due to heat transfer (boiling and condensation) [2–4]. This has attracted attention as a means of removing heat from microprocessors in computers [5]. To understand convective boiling in microchannels, single and multiple channel structures have been developed using conventional machining [6, 7] and silicon micromachining [4, 6–12].

With the promises of performance gains in PEMFC by using microchannels (0.05–1 mm) to improve gas routing [13], two-phase flow in microchannels has become a leading topic of interest within the fuel cell community. The complexities of water management have been previously investigated [14–16]; however, most studies have focused on the issue of water flow and transport only in the Membrane Electrode Assembly (MEA) and Gas Diffusion Layer (GDL). Very few studies have been directed toward the understanding of flow behavior in microchannels, and most are theoretical or computational in nature [17, 18]. Experimental work related to two-phase flow in fuel cell channels is limited and relates mainly to minichannels (mm size) [19] and direct methanol fuel cell systems, with low void fractions [20].

In this paper, the work on two-phase flow being carried out at the Micro Heat Transfer Laboratory (MHTL) at Stanford is reviewed, with a specific focus on the advances in imaging, metrology, and modeling of microchannels for microchip cooling and fuel cell applications. Task-specific samples are manufactured employing microfabrication technology that enables the imaging and integration of distributed sensing elements. White light- and fluorescence-based techniques are employed in order to characterize flow behavior and structure. They allow for film thickness, liquid volume fraction, and velocity fields measurements, among other things. The samples integrate heaters and temperature sensors for heat and mass transfer characterization. The thermistors can be made using either a metal, such as aluminum, or by selectively doping the silicon substrate. The experimental work is complemented by modeling the convective heat transfer and fluid mechanics of the flows.

MICROCHANNEL DESIGN AND FABRICATION

Depending on the specific application, microchannels for each particular task have their own specific requirements that make their fabrication unique. They do, however, share a lot of common microfabrication processing ground. Microchip cooling test samples focus on the convective heat transfer nature of the flow, and, as such, require special handling and characterization of the heat flow. These channels are fabricated in a suspended beam architecture that limits the amount of axial conduction losses [21]. In this manner, the applied heat can be confined to the channel region, and more accurate estimates of the actual convective heat transfer and transport due to fluid flow and phase change can be obtained (see Figure 1).

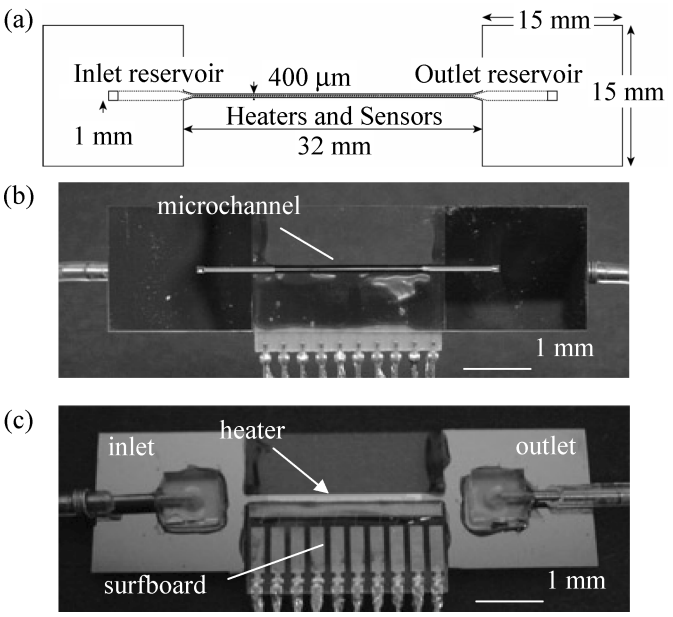

Figure 1 (a) Schematic test device showing suspended microchannel with inlet and outlet reservoirs. (b) Front side photograph of final structure showing suspended channel, reservoirs, and surfboards attached to pyrex. (c) Back side photograph showing heater side along with inlet and outlet fluidic ports.

In the case of microchannels for fuel cell applications, the main focus is shifted from the heat transfer aspect of the flow toward the mass transport and liquid entrainment effects on flow behavior. Of course, any study that involves mass transport due to phase change requires an understanding of the heat transfer characteristics of the system, and such an understanding of the heat transfer plays an important role. For these particular studies, it was important to achieve a controlled introduction of liquid water into the flow stream. Thus, samples are fabricated with distributed water injection slots or channels (see Figure 2). The architecture of the injection geometry allows for varied studies, where a single injection slot sample can be used to isolate the mechanics of droplet entrainment, while more involved geometry incorporating multiple injection slots are useful in understanding the global interactions of the liquid with the gas [22].

Both types of samples incorporate integrated temperature sensing and heating capabilities. The heaters are fabricated by depositing aluminum as resistive elements. Temperature sensors consist of either deposited aluminum or doped silicon. Resistance temperature detectors (RTDs) are based on the natural change in the sensor's resistance with temperature. The temperature coefficient of resistance (TCR) symbolizes the resistance change factor per degree of temperature change [23].

The fabrication of both types of samples relies heavily on the use of Deep Reactive Ion Etching (DRIE) to carve out the microchannels in a silicon substrate. Selective metal (aluminum) deposition or silicon doping by means of lithography is the backbone for the fabrication of temperature sensors on the opposite side of the substrate. Optical access is achieved with the anodic bonding of Pyrex glass to seal the etched microchannels.

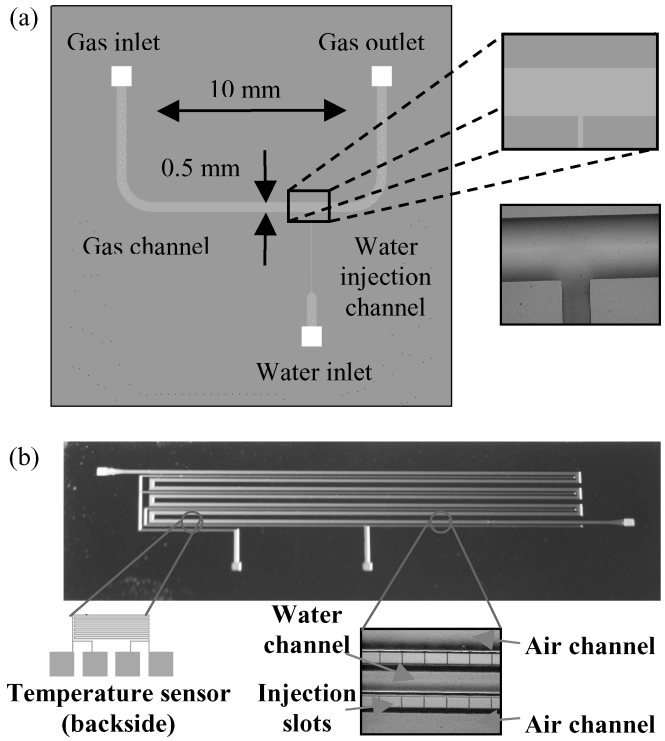

Figure 2 Distributed water injection test structures for fuel cell applications: (a) first-generation structure with a single water injection slot; (b) second-generation structure incorporating serpentine geometry, distributed water injection throughout its entire length, and temperature sensors in the backside.

The overall process flow for a full structure consists of the following steps (see Figure 3):

1. 1500 Å of thermal oxide is grown as an electrical insulated layer.
2. 0.5 μm of aluminum is deposited and patterned on the back surface as the heaters and thermistors. When implementing silicon-doped temperature sensors, a previous lithography step is carried out for selective ion implantation.
3. 2000 Å of low-temperature oxide (LTO) is deposited to protect heaters and temperature sensors.
4. The contacts of heaters and sensors for wire bonding are opened through pad-etching and holes for air/water inlets and outlets are opened with through-etching. Oxide in the front side is also etched away in this step.
5. To create the distributed water injection layout in the fuel cell application channels, silicon is etched 5 μm deep for water injection channels by DRIE.
6. Silicon is etched 200 μm deep by DRIE to create the main channel.
7. Holes for air/water inlets and outlets are etched through. For the microchannel cooling test samples, this step is also used to etch away the majority of silicon material surrounding the microchannel. This creates the suspended and isolated beam structure that constrains heat flux to the channel itself with minimal conduction losses to the substrate.
8. Pyrex glass is anodically bonded to the top of the silicon to provide optical access of the flow.

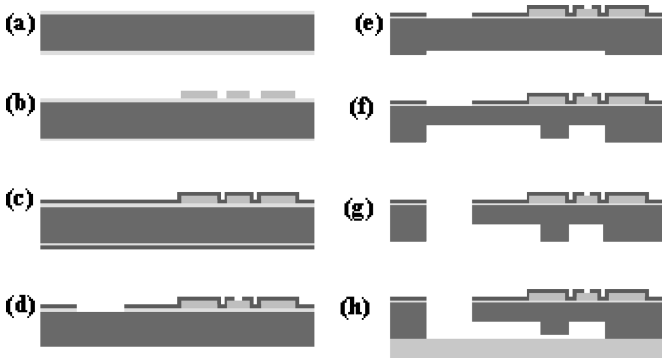

Figure 3 Microfabrication process: (a) growing of thermal oxide; (b) aluminum deposition and patterning on back surface; (c) protective low temperature oxide (LTO) deposition; (d) pad-etching to open contacts and front oxide etching; (e) Deep Reactive Ion Etching (DRIE) of water injection slots; (f) DRIE of air and water channels; (g) etching through holes for air/water inlets and outlets; (h) anodic bonding of pyrex glass on the top of the silicon.

OPTICAL CHARACTERIZATION

Optical characterization of the flows is mainly achieved through the use of white light and fluorescent imaging. Besides flow structure classification, the optical techniques employed allow the quantification of flow parameters such as film thickness, liquid fraction, and velocity. At the heart of these measurements is a Nikon TE2000U inverted epifluorescence microscope system, which can also be used in white light mode. A Roper Scientific 12-bit CoolSNAP ES CCD camera is used for image capture with 4X and 10X objectives. A metal halide lamp and appropriate filter cubes are used for fluorescence purposes (mainly Fluorescein) [22]. Figure 4 shows a schematic of the microscope configuration in fluorescence mode.

Fluorescence is a photoluminescence process by which a fluorophore molecule (fluorescent dye) absorbs light of a certain wavelength (color) and subsequently emits light of longer

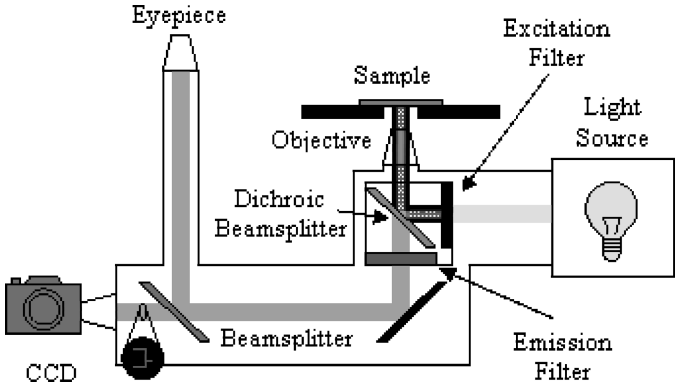

Figure 4 Epifluorescence microscope imaging setup.

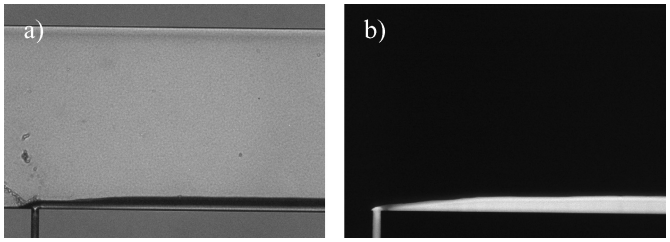

Figure 5 Comparison of (a) white light and (b) fluorescence imaging of the water film in the microchannel.

wavelength (lower energy). This difference in color between the absorbed (exciting) and emitted light allows for very distinctive imaging, as the fluorescence becomes a tracer. In most instances, fluorescence tracking of the liquid phase is achieved by mixing an appropriate fluorophore with water. In other instances, such as μPIV, the tracking of fluorescent particles seeded into the flow is used to infer properties of the flow such as velocity.

In stratified two-phase flow, fluorescence is used to accurately determine the extent of the liquid phase [24]. Fluorescein is used to track where the water is. Figure 5 shows a water film imaged with (a) white light and (b) fluorescence. The air-water and water-channel interfaces are clearer and more distinguishable in the fluorescence image. This clarity allows the images to be used for accurate, quantitative measurements of the film extent (thickness) in the plane of the image, which are made by counting the number of pixels that are brightened by fluorescence. The pixels are counted according to whether the brightness of that pixel exceeds certain threshold brightness. To measure the film thickness in the y-direction, pixels above the threshold brightness in each column of pixels are counted and added up. This number is multiplied by the vertical dimension of a pixel to obtain the film thickness. Figure 6 shows a plot of film thickness versus pressure drop obtained using this technique.

Fluorescence is also used for high-speed, spatially averaged, liquid fraction measurements [25]. Just as in the case of film thickness measurements, fluorescein is used for water tracking purposes. However, the CCD in the epifluorescence system is replaced by a photodiode with a much faster response time and the capability for short transient measurements. The signal of the photodiode is proportional to the total fluorescence emitted from within the field of view of the microscope. As such, it is also indicative of the liquid fraction. The system is calibrated with the use of a CCD for actual spatial measurements of void fraction. Figure 7 shows a typical signal from the photodiode for a flow with a time-averaged liquid fraction of 0.5. Figure 8 shows actual measurements obtained from this technique for flows with different time-averaged liquid fractions. The validity and accuracy of this technique are evident from this plot.

Another technique based on the use of fluorescence is μPIV. It allows liquid velocity field measurements, something of particular interest during bubble growth in a heated microchannel

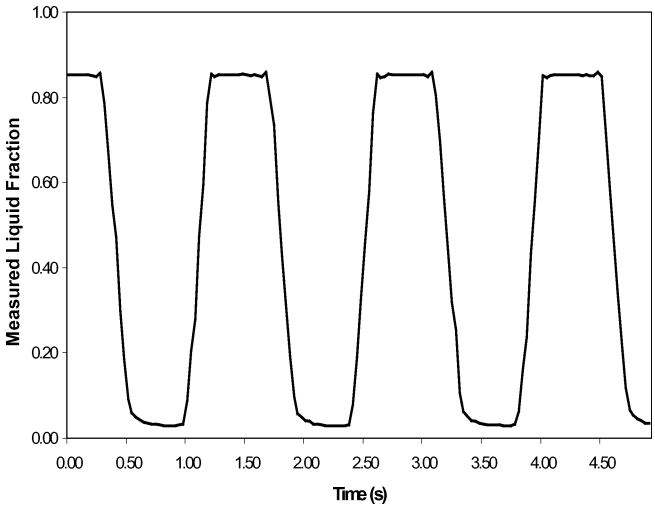

Figure 7 A portion of the transient signal for a run in which the predicted average liquid fraction is 0.5.

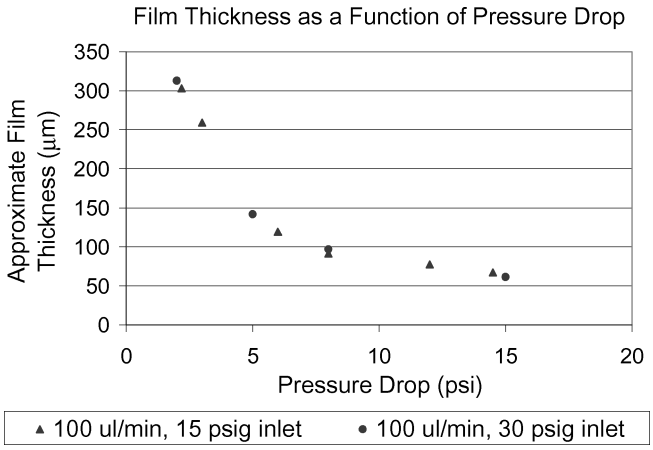

Figure 6 Film thickness as a function of pressure drop across the channel for water flow rate of 100 μL/min.

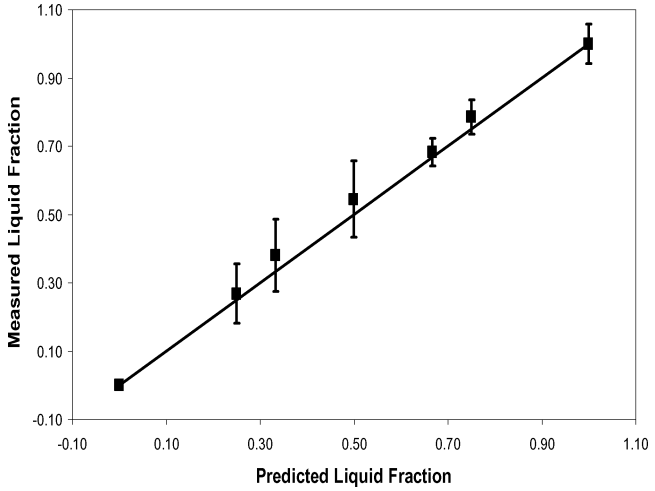

Figure 8 Comparison of the time-averaged liquid fraction measured by the photodiode to the predicted delivered void fraction.

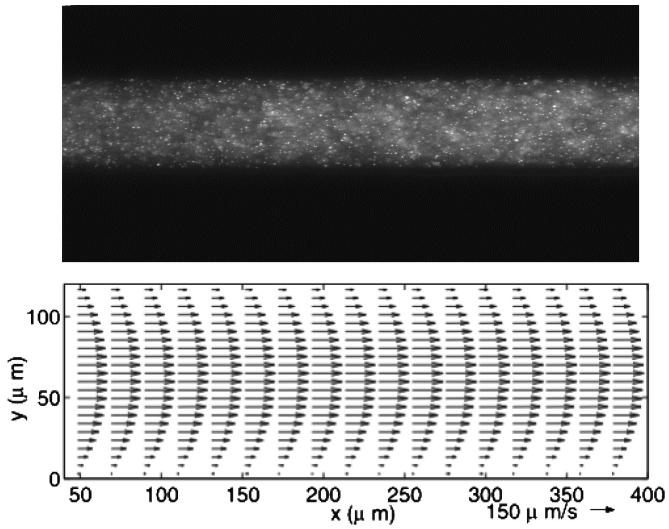

Figure 9 Typical μPIV image and velocity vector field obtained for a single-phase liquid flow in a microchannel.

[26]. The working fluid (deionized water) is seeded with 0.7 μm fluorescent particles to a volume density of 0.025%. The particles (Duke Scientific) have a peak excitation wavelength in blue ($\lambda = 468$ nm) and a peak emission wavelength in green ($\lambda = 508$ nm). A pulsed laser is used to excite the particles while a synchronized scientific CCD captures the fluorescence emissions coming from the particles. These fluorescence images contain information regarding the particle's spatial distribution in the flow. An image cross-correlation algorithm is used to track the movement of particles from one image to the next to determine the flow displacement fields and, consequently, velocity fields. Figure 9 shows a typical μPIV image and velocity vector field obtained for single-phase liquid flow in a microchannel.

MODELING

There are two approaches to modeling liquid-vapor two-phase flows. The first, the *homogeneous model*, treats the flow as a homogenous fluid [27] with properties that are the mass-weighted averages of the local properties of the liquid and the vapor. These properties are used to evaluate the incompressible Navier-Stokes and energy equations for a single fluid [28].

$$\frac{d}{dz}(\overline{\rho u}) = \frac{\delta \dot{m}}{A} \tag{1}$$

where $\delta \dot{m}$ accounts for the formation and introduction of liquid water into the flow, as is the case for microchannels in the cathode side of fuel cells. This liquid water addition is treated as a source term. In two-phase boiling flows, this term would be equal to zero. The momentum and energy equations for the homogeneous model are:

$$\frac{d}{dz}(\bar{\rho} u^2) = -\frac{dp}{dz} - \frac{P_w}{A}\bar{\tau}_w \tag{2}$$

$$\frac{d}{dz}\left(\bar{\rho}\left[\bar{h} + \frac{\bar{u}^2}{2}\right]\bar{u}\right) = \frac{h_{conv} P_h}{A}(T_s - T_f) + \frac{h_m \delta \dot{m}}{A} \tag{3}$$

The homogeneous model limits the physics that can be incorporated into the model. The two phases are considered to be uniformly distributed within each grid element. Local temperature and pressure differences between phases cannot be captured by treating the two phases as a homogenous fluid.

On the other hand, *separated flow models* incorporating interface exchanges have been introduced to permit different gas and liquid velocities and flow directions as well as different liquid and gas temperatures [4]. These models still rely on one-dimensional formulations and spatial averaging. In other words, they do not consider fluid variation of properties (e.g., velocity and temperature) and their gradients at the interfaces or at the wall boundaries. Such two-fluid models therefore require closure laws to deal with the interfaces as well as the wall boundary conditions. Because these closure laws are known to depend on flow patterns, flow regime maps must also be specified. The generalized two-phasic mass, momentum, and energy conservation formulations for a separated flow model are given by

$$\frac{\partial}{\partial z}[\rho_G \bar{\alpha} \bar{u}_G] = \Gamma \tag{4}$$

$$\frac{\partial}{\partial z}[\rho_L (1 - \bar{\alpha}) \bar{u}_L] = -\Gamma + \frac{\delta \dot{m}}{A} \tag{5}$$

where

$$\bar{u}_G = \frac{1}{A_G}\int_{A_G} u_G dA_G = \frac{G_G}{\bar{\alpha}\rho_G} \tag{6}$$

$$\bar{u}_L = \frac{1}{A_L}\int_{A_L} u_L dA_L = \frac{G_L}{(1 - \bar{\alpha})\rho_L} \tag{7}$$

are the average liquid and gas velocities, and G_G and G_L are the mass flow rates of gas and liquid per unit area.

Equation (4) allows for some of the fluid to be transferred (or converted) into the gas (or vapor) phase at the rate Γ per unit volume. Some of that transfer can occur at the wall and the rest at the interface.

The corresponding phasic momentum equations are:

$$\frac{\partial}{\partial z}\left[\rho_G \bar{\alpha} \bar{u}_G^2\right] = -\bar{\alpha}\frac{\partial p}{\partial z} - \frac{P_{wG}\tau_{wG}}{A} - \frac{P_i \tau_i}{A} + \Gamma \bar{u}_{iG} \tag{8}$$

$$\frac{\partial}{\partial z}\left[\rho_L (1 - \bar{\alpha}) \bar{u}_L^2\right] = -(1 - \bar{\alpha})\frac{\partial p}{\partial z} - \frac{P_{wL}\tau_{wL}}{A} + \frac{P_i \tau_i}{A} - \Gamma \bar{u}_{iL} \tag{9}$$

The terms on the right side of Eqs. (8) and (9) are the forces on phase k, where k can represent the liquid phase L or the gas phase G. The first term on the right side of Eqs. (8) and (9) is the net pressure force acting on phase k. The second and third terms are the shear stresses acting on the phase at the wall and at the interface, and they are denoted respectively by τ_{wk} and τ_i. The parameter P_{wk} is the part of the wall perimeter wetted by phase k. The next term on the right side represents the momentum

addition into phase k by the mass exchange at the interface. The mass entering phase k has an interface velocity $\bar{u}_{ik}$.

The corresponding phasic energy equations can be written in terms of total enthalpy $H_k = h_k + \bar{u}_k^2/2$, which leads to:

$$\frac{\partial}{\partial z}[\rho_G \bar{\alpha} \bar{H}_G \bar{u}_G] = \frac{q''_{iG} P_i}{A} + \frac{q''_{wG} P_{hG}}{A} + \Gamma \bar{H}_{iG} + \xi \frac{P_i}{A} \tau_i \bar{u}_{iG} \quad (10)$$

$$\frac{\partial}{\partial z}[\rho_L (1 - \bar{\alpha}) \bar{H}_L \bar{u}_L] = \frac{q''_{iL} P_i}{A} + \frac{q''_{wL} P_{hL}}{A} - \Gamma \bar{H}_{iL} - \xi \frac{P_i}{A} \tau_i \bar{u}_{iL} \quad (11)$$

The first and second terms on the right-hand side of Eqs. (10) and (11) are the sensible heat inputs from the interfacial perimeter P_i and from the heated portion of the perimeter wetted by phase k, P_{hK}. The third term accounts for energy addition to phase k due to interfacial mass transfer, with $\bar{H}_{ik}$ being the total enthalpy characteristic of this exchange. The last term is related to the interfacial energy dissipation. The parameter ξ represents the fraction of energy dissipated at the interface that gets transferred to the gas phase. For the case of microchannel cooling of integrated circuits, where heat transfer is the most relevant parameter, the energy balance equation must be extended to incorporate conduction in the solid as a boundary condition. This leads to a conjugate problem that must be simultaneously solved for the temperatures in the flow as well as in the solid.

In order to properly and formally solve the conservation equations, formulations must be established for the exchange terms between the two phases and their boundaries. This is the basis behind the Lockhart-Martinelli correlations and parameters, which are usually determined by fitting experimental data and are dependent on flow regime. Our approach has been to formulate physics-based correlations for the different flow regimes. We use the exact analytical solutions from simple flows to extract approximations for the correlations of more complicated flows and geometries that do not lend themselves to simple formulations. Thus, rather than formulating correlations from experimental data fitting, an *ab initio* approach is used and the experimental data are checked for validation.

RESULTS AND DISCUSSION

The wealth of experimental and modeling work has allowed the characterization of some interesting phenomena in two-phase flows for both microchannel cooling and fuel cell water management applications. Axial temperature distribution [4], stratified flow film thickness [22, 24], and water slug detachment criteria [29] are among the critical parameters investigated for these applications.

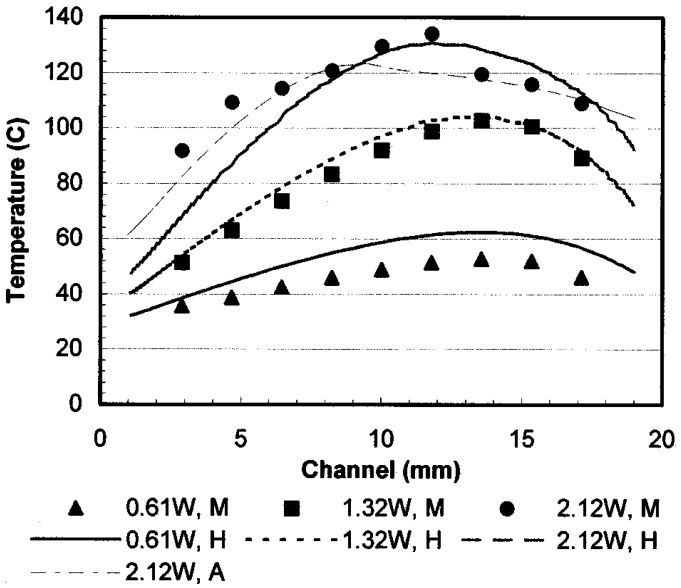

Figure 10 Temperature profile for a single 50 μm-wide by 70 μm-deep by 20 mm-long microchannel under different input powers and flow rate of 0.1 mL/min.

Figure 10 shows a comparison of the experimental and simulated temperature profiles for a single 50 μm-wide by 70 μm-deep by 20 mm-long microchannel under different input powers and a flow rate of 0.1 mL/min [4]. The agreement between the two is extremely good. Notice that at low input powers of 0.61 W and 1.32 W, the homogeneous model is sufficient to capture the physics associated with the temperature profile. However, for the high input power of 2.12 W, a separated flow model based on the annular flow regime does a better job of simulating the temperature distribution along the channel. This can be better understood by looking at the actual temperature values attained in the channel. For the low input powers, the temperature barely reaches 100°C, meaning there is very little boiling. Consequently, the flow is mainly liquid and can be accurately modeled as a homogeneous flow. Conversely, for the high input power, the temperatures throughout the channel are above the boiling point of water. This leads to the presence of a lot of water vapor in the flow. The physics of this type of flow are better captured with a separated two-phase flow formulation, of an annular fashion in this particular case.

Another parameter of extreme importance in the performance of microchannel cooling systems is the pressure drop [4]. Figure 11 shows a comparison of the measured pressure drop versus that obtained from the homogeneous and annular (separated) two-phase flow models as a function of input power. Again, the agreement between the experimental data and models is quite good. Initially, the pressure drop decreases as the power is increased. This is a consequence of the decrease in water viscosity due to the increase of liquid temperature with heat. In this region, the flow is strictly single phase (liquid water), and as such both the homogeneous and annular formulations collapse to produce exactly the same result. Above a value of around 1.30 W, a further increase in the input power produces

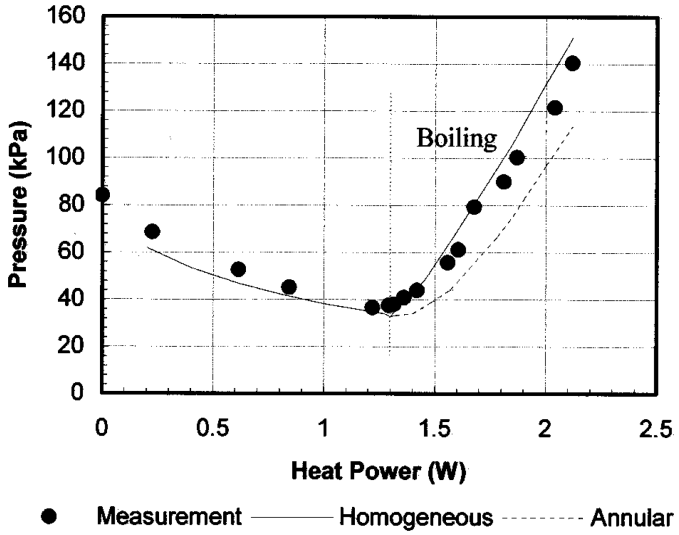

Figure 11 Pressure drop as a function of input power for a single 50 μm-wide by 70 μm-deep by 20 mm-long microchannel for a flow rate of 0.1 L/min.

an increase in pressure drop. This behavior corresponds to the onset and continuance of boiling. The increase in pressure results from the change in phase and required acceleration of the low-density vapor to preserve mass conservation.

Knowledge of stratified flow is also important in fuel cell applications, albeit in a different fashion [22, 24]. The performance of the fuel cell is not only affected by the overall pressure drop in the channel but also by the reduction in effective area for air flow resulting from the introduction of liquid water. Thus, predicting the extent of the liquid phase in a stratified flow configuration is key in the determination of air flow rate and, consequently, current output. Figure 12 shows a comparison of the experimental and simulated stratified flow film thickness as a function of inlet air velocity for a 500 μm-wide by 45 μm-deep microchannel under a water injection rate of 100 μL/min [22, 24]. The experimental data were obtained using the fluorescence technique already described. The simulation film thickness was computed using the separated flow model with different closure laws formulations for a stratified flow. The agreement between the model using hybrid friction factor formulations and experimental data is quite good. As expected, film thickness decreases with an increased pressure drop and air flow rate in the channel. Notice that for inlet velocity below 5 m/s, the film thickness is more than half the total width of the channel (500 μm). This represents a substantial decrease in the effective air flow area with detrimental consequences in fuel cell performance.

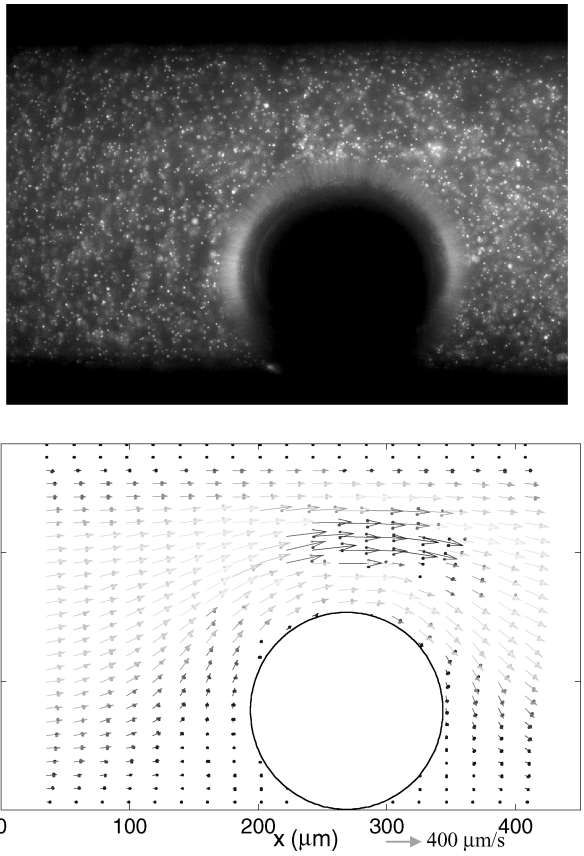

Figure 13 Velocity field around a departing bubble in a heated microchannel obtained using the μPIV technique.

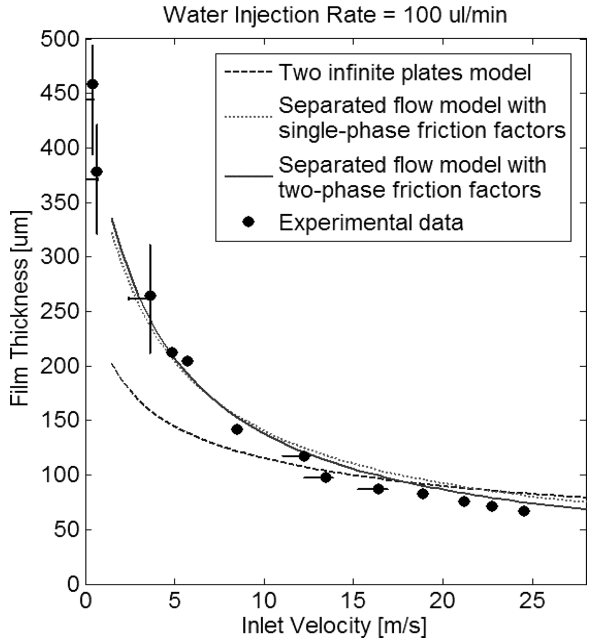

Figure 12 Film thickness versus inlet air flow velocity. The different model simulations correspond to different formulations of the friction factor correlations.

Of equal importance in two-phase flow are the detachment criteria for bubbles and droplets [26, 29]. It is important to understand under what conditions bubbles (in boiling) or droplets (in fuel cell water formation) that grow from the channel walls will get entrained into the flow. These detachment criteria are important because if the bubble or droplet gets to grow as big as the channel size before being removed, it leads to the formation of dry out slugs and water plugs in the cooling and fuel cell microchannels, respectively. These two conditions seriously reduce the performance brought about by microchannel use in

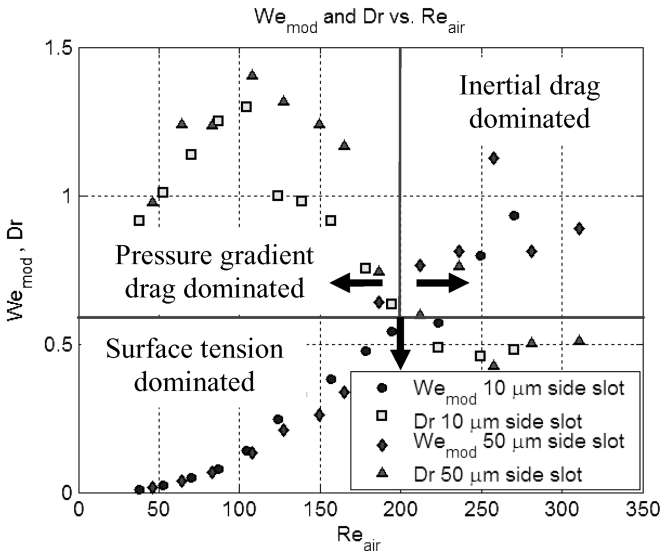

Figure 14 Droplet detachment regimes and transition point.

these two technologies. In the case of microchannel boiling, μPIV is being used to study the forces imposed on the bubbles by the flow that can lead to detachment [26]. Figure 13 shows a μPIV image of the flow around the bubble and the corresponding velocity vectors. We are currently using these velocity fields in conjunction with numerical simulations to determine the drag forces imposed on the bubble. Similarly, we are investigating droplet detachment in hydrophobic channels for fuel cell applications [29]. Correlations between air flow conditions (pressure drop, velocity) and droplet geometry (size, contact angle) have been established and used as the foundation for the creation of a detachment regime map (see Figure 14). Pressure gradient and inertial (form) drag are recognized as the two major contributors to droplet detachment in this map. Whenever one (or both) of these forces overcomes surface tension, droplet detachment occurs. The transition from the pressure gradient-dominated regime to the inertial drag-dominated one occurs at $\mathrm{Re} = 200$.

SUMMARY AND CONCLUSIONS

This manuscript summarizes progress on two-phase flow in microchannels performed at the Stanford Micro Heat Transfer Laboratory (MHTL). The work described here focuses on developing a fundamental understanding of two-phase boiling flows in microchannels for integrated circuit cooling as well as flow behavior and transport for liquid water management in fuel cell applications. The work encompasses the use of novel microfabricated samples with integrated sensory capabilities and matching first-order modeling of the different phenomena under investigation. Experimental studies have relied heavily on the use of optical diagnostics techniques to characterize the different flow regimes observed. Among the parameters measured are "quasi-instantaneous" liquid fraction, film thickness, and velocity fields. The simulation side has relied heavily on the use and further development of homogeneous and separated two-phase flow models with an emphasis on the formulation of physics based closure laws.

This combined approach has allowed the characterization of temperature distribution and pressure drop in microchannel boiling under different heat input conditions. Likewise, the characterization of the extent of film thickness under different water and air flow conditions in stratified two-phase flow has been extensively studied. Finally, the detachment criteria leading to the removal of bubbles and droplets from the channel walls have been investigated. Further work in the area of two-phase flow is needed, particularly in terms of transient phenomena.

NOMENCLATURE

A	cross-sectional area, m^2
f	friction factor
G	$= \rho u$, mass flow rate per unit area, kg/s-m^2
H	$= h + u^2/2$, total enthalpy per unit mass, J/kg
h	enthalpy per unit mass, J/kg
h_{conv}	convective heat transfer coefficient, W/m^2-K
h_m	liquid water enthalpy, J/kg
k	thermal conductivity, W/m-K
$\dot{m}$	$= \rho u A$, mass flow rate, kg/s
$\delta\dot{m}$	water injection mass flow rate, kg/s
P	channel perimeter, m
P_h	heated perimeter, m
P_w	wetted perimeter, m
p	pressure, Pa
Q	$= uA$, volumetric flow rate, m^3/s
q''	heat flux, W/m^2
T	temperature, K
T_f	fluid temperature, K
T_s	channel wall temperature, K
u	axial velocity, m/s
z	axial direction, m

Greek Symbols

α	gas volume fraction
Γ	mass transfer rate per unit volume, kg/s-m^3
μ	dynamic viscosity, Pa-s
ρ	density, kg/ m^3
τ	shear stress, Pa
ξ	energy fraction dissipated at the two fluids interface

REFERENCES

[1] Kandlikar, S. G., ed., *Proc. First International Conference on Microchannels and Minichannels*, Rochester, NY, April 24–25, 2003.

[2] Kandlikar, S. G., and Balasubramanian, P., An Extension of the Flow Boiling Correlation to Transition, Laminar, and Deep Laminar Flows and Microchannels, *Heat Transfer Engineering,* vol. 25, no. 3, pp. 86–93, 2004.

[3] Stanley, R. S., and Barron, R. F., Two-Phase Flow in Microchannels, *Microelectromechanical Systems (MEMS): Proc. 1997 ASME International Mechanical Engineering Congress and Exposition,* Dallas, Tex., November 16–21, 1997.

[4] Zhang, L., Koo, J.-M., Jiang, L., Asheghi, M., Goodson, K. E., Santiago, J. G., and Kenny, T. W., Measurements and Modeling of Two-Phase Flow in Microchannels with Nearly Constant Heat Flux Boundary Conditions, *Journal of Microelectromechanical Systems*, vol. 11, no. 1, pp. 12–19, 2002.

[5] Jiang, L., Mikkelsen, J., Koo, J.-M., Huber, D., Yao, S., Zhang, L., Zhou, P., Maveety, J. G., Prasher, R., Santiago, J. G., Kenny, T. W., and Goodson, K. E., Closed-Loop Electroosmotic Microchannel Cooling System for VLSI Circuits, *IEEE Transactions on Components and Packaging Technologies*, vol. 25, no. 3, pp. 347–355, 2002.

[6] Peng, X. F., and Wang, B.-X., Forced Convection and Flow Boiling Heat Transfer for Liquid Flowing through Microchannels, *International Journal of Heat and Mass Transfer*, vol. 36, no. 14, pp. 3421–3427, 1993.

[7] Peng, X. F., Hu, H. Y., and Want, B. X., Flow Boiling through V-Shape Microchannels, *Experimental Heat Transfer*, vol. 11, no. 1, pp. 87–100, 1998.

[8] Hetsroni, G., Mosyak, A., and Segal, Z., Nonuniform Temperature Distribution in Electronic Devices Cooled by Flow in Parallel Microchannels, *IEEE Transactions on Components and Packaging Technologies*, vol. 24, no. 1, pp. 16–23, 2001.

[9] Jiang, L., Wong, M., and Zohar, Y., 2000, Phase Change in Microchannel Heat Sink under Forced Convective Boiling, *Proc. 13th Annual International Conference on Micro Electro Mechanical Systems*, Miyazaki, Japan, January 23–27, 2000.

[10] Lee, M., Wong, Y. Y., Wong, M., and Zohar, Y., Size and Shape Effects on Two-Phase Flow Patterns in Microchannel Forced Convection Boiling, *Journal of Micromechanics and Microengineering*, vol. 13, no. 1, pp. 155–164, 2003.

[11] Peles, Y. P., Yarin, L. P., and Hetsroni, G., Steady and Unsteady Flow in a Heated Capillary, *International Journal of Multiphase Flow*, vol. 27, no. 4, pp. 577–598, 2001.

[12] Zhang, L., Koo, J.-M., Jiang, L., Goodson, K. E., Santiago, J. G., and Kenny, T. W., Study of Boiling Regimes and Transient Signal Measurements in Microchannels, *Proc. 11th International Conference on Solid-State Sensors and Actuators*, Munich, Germany, June 10–14, 2001.

[13] Cha, S. W., Lee, S. J., Park, Y. I., and Prinz, F. B., Investigation of Transport Phenomena in Micro Flow Channels for Miniature Fuel Cells, *Proc. 1st International Conference on Fuel Cell Science, Engineering and Technology*, New York, NY, April 21–23, 2003.

[14] Berg, P., Promislow, K., Pierre, J. St., Stumper, J., and Wetton, B., Water Management in PEM Fuel Cells, *Journal of the Electrochemical Society*, vol. 151, no. 3, pp. A341–A353, 2004.

[15] Wang, Z. H., Wang, C. Y., and Chen, K. S., Two-Phase Flow and Transport in the Air Cathode of Proton Exchange Membrane Fuel Cells, *Journal of Power Sources*, vol. 94, no. 1, pp. 40–50, 2001.

[16] You, L., and Liu, H., A Two-Phase Flow and Transport Model for the Cathode of PEM Fuel Cells, *International Journal of Heat and Mass Transfer*, vol. 45, no. 11, pp. 2277–2287, 2002.

[17] Yuan, J., Rokni, M., and Sundén, B., Simulation of Fully Developed Laminar Heat and Mass Transfer in Fuel Cell Ducts with Different Cross Section, *International Journal of Heat and Mass Transfer*, vol. 44, no. 21, pp. 4047–4058, 2001.

[18] Yuan, J., Rokni, M., and Sundén, B., Modeling of Two-Phase Flow in a Cathode Duct of PEM Fuel Cells, *Fuel Cell Science, Engineering and Technology: Proc. 1st International Conference on Fuel Cell Science, Engineering and Technology*, Rochester, NY, April 21–23, 2003.

[19] Mench, M. M., Dong, Q. L., and Wang, C. Y., In Situ Water Distribution Measurements in a Polymer Electrolyte Fuel Cell, *Journal of Power Sources*, vol. 124, no.1, pp. 90–98, 2003.

[20] Yang, H., Zhao, T. S., and Cheng, P., Characteristics of Gas-Liquid Two-Phase Flow Patterns in Miniature Channel Having a Gas Permeable Sidewall, *Proc. IMECE 2002: ASME International Mechanical Engineering Congress & Exposition*, New Orleans, La., November 17–22, 2002.

[21] Kramer, T. A., Flynn, R. D., Fogg, D. W., Wang, E. N., Hidrovo, C. H., Prasher, R. S., Chau, D. S., Narasimhan, S., and Goodson, K. E., Microcahnnel Experimental Structure for Measuring Temperature Fields during Convective Boiling, *Proc. IMECE 2004: ASME International Mechanical Engineering Congress & Exposition*, Anaheim, Calif., November 13–20, 2004.

[22] Hidrovo, C. H., Wang, F.-M., Lee, E. S., Vigneron, S., Steinbrenner, J. E., Paidipati, J. V., Kramer, T. A., Eaton, J. K., and Goodson, K. E., Experimental Investigation and Visualization of Two-Phase Flow and Water Transport in Microchannels, *Proc. IMECE 2004: ASME International Mechanical Engineering Congress & Exposition*, Anaheim, Calif., November 13–20, 2004.

[23] Wang, F.-M., Steinbrenner, J. E., Hidrovo, C. H., Kramer, T. A., Lee, E. S., Vigneron, S., Cheng, C.-H., Eaton, J. K., and Goodson, K. E., Investigation of Two-Phase Transport Phenomena in Microchannels Using a Microfabricated Experimental Structure, *Proc. Heat Transfer in Components and Systems for Sustainable Energy Technologies: Heat-SET 2005*, Grenoble, France, April 5–7, 2005.

[24] Steinbrenner, J. E., Hidrovo, C. H., Wang, F.-M., Vigneron, S., Lee, E. S., Kramer, T. A., Cheng, C.-H., Eaton, J. K., and Goodson, K. E., Measurement and Modeling of Liquid Film Thickness Evolution in Stratified Two-Phase Microchannel Flows, *Proc. Heat Transfer in Components and Systems for Sustainable Energy Technologies: Heat-SET2005*, Grenoble, France, April 5–7, 2005.

[25] Fogg, D., Flynn, R., Hidrovo, C., Zhang, L., and Goodson, K., Fluorescent Imaging of Void Fraction in Two-Phase Microchannels, *Proc. 3rd International Symposium on Two-Phase Flow Modeling and Experimentation*, Pisa, Italy, September 22–24, 2004.

[26] Wang, E. N., Devasenathipathy, S., Hidrovo, C. H., Fogg, D. W., Koo, J.-M., Santiago, J. G., Goodson, K. E., and Kenny, T. W., Liquid Velocity Field Measurements in Two-Phase Microchannel Convection, *Proc. 3rd International Symposium on Two-Phase Flow Modeling and Experimentation*, Pisa, Italy, September 22–24, 2004.

[27] Levy, S., *Two-Phase Flow in Complex Systems,* Wiley-Interscience, New York, 1999.

[28] Vigneron, S., Hidrovo, C. H., Wang, F.-M., Lee, E. S., Steinbrenner, J. E., Kramer, T. A., Eaton, J. K., and Goodson, K. E., 1D Homogeneous Modeling of Microchannel Two-Phase Flow with Distributed Liquid Water Injection from Walls, *Proc. IMECE*

2004: ASME International Mechanical Engineering Congress & Exposition, Anaheim, Calif., November 13–20, 2004.

[29] Hidrovo, C. H., Wang, F.-M., Steinbrenner, J. E., Lee, E. S., Vigneron, Cheng, C.-H., Eaton, J. K., and Goodson, K. E., Water Slug Detachment in Two-Phase Hydrophobic Microchannel Flows, *Proc. ICMM2005: 3rd International Conference on Microchannels and Minichannels,* Toronto, Ontario, Canada, June 13–15, 2005.

Carlos Hidrovo received his B.S. degree (1995) from MIT, his M.S. degree (1996) from UIUC, and his Ph.D. degree (2001) from MIT, all in mechanical engineering. As a Ph.D. student, he was a member of the Hatsopoulos Microfluids Laboratory and worked on tribology, lubrication, and fluorescence-based optical diagnostics. This latter work earned him the ASME 2001 Robert T. Knapp Award. He was a research scientist in the Optical Engineering Laboratory at MIT from 2001 to 2003. He is currently a research associate in the Microscale Heat Transfer Laboratory at Stanford University working toward the understanding of microscale two-phase flow and water transport in PEM fuel cells.

Theresa A. Kramer received her B.S. degree (1995) from Yale University and her M.S. (1997) and Ph.D. degrees (2003) from Stanford University, all in applied physics. She was a postdoctoral scholar at Stanford University from 2003 to 2004, where she worked on the microfabrication of microchannel structures for microprocessor cooling applications and for the characterization of two-phase flow in fuel cell microstructures. She is now with Applied Materials in Santa Clara, California.

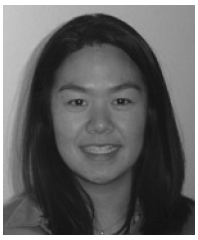

Evelyn N. Wang received her B.S. degree from M.I.T. in 2000 and her M.S. degree from Stanford University in 2001 in mechanical engineering. Currently, she is working toward her Ph.D. in the mechanical engineering department at Stanford University with support from the National Defense Science Graduate Fellowship. Her research interests include MEMS-based thermal management for high-power applications and the advanced packaging of IC chips.

Sébastien Vigneron received his B.S. degree in mechanical engineering (2002) and his M.S. degree in Applied Mathematics (2003), both from Ecole Polytechnique in France, and a second M.S. degree in Aeronautics & Astronautics from Stanford University. At Stanford, he worked on modeling two-phase flow in a microchannel with a porous wall for PEM fuel cell water management applications. He is currently working with Dassault-Aviation in France on the aerodynamic design of a supersonic business jet.

Julie Steinbrenner is pursuing a Ph.D. in mechanical engineering at Stanford University under Prof. Kenneth Goodson. She earned her B.S.M.E. at Valparaiso University, Indiana (2002) and her M.S.M.E. at Stanford University (2004). Interested in global energy issues and technologies, she enjoyed researching solar energy technologies at the Paul Scherrer Institut in Switzerland and at CNRS-Odeillo, France. She is currently working to characterize thermal and hydrodynamic aspects of two-phase flow in microchannels for PEM fuel cell applications. Her work is sponsored by Honda Research & Development, Co. and the Charles H. Kruger Stanford Graduate Fellowship.

Jae-Mo Koo received his B.S. and M.S. degrees in Mechanical Engineering from Hongik University, Seoul, Korea, in 1994 and 1996, respectively. From 1997 to 1998, he worked for the Korea Institute of Science and Technology, Seoul, Korea. He received his M.S. degree from the University of Wisconsin, Madison, in mechanical engineering in 1999. Currently, he is working toward the doctoral degree at Mechanical Engineering Department, Stanford University. His research interests are microscale heat transfer, micro-fluidics, MEMS, advanced electronic cooling technology, and electronic/MEMS packaging.

Fu-Min Wang received his B.S. (1993) and M.S. (1995) in mechanical engineering from National Taiwan University. He received his second M.S. (2000), majoring in MEMS and specializing in microscale heat transport phenomena, from the Mechanical and Aerospace Engineering Department at UCLA. He is working toward his Ph.D. in mechanical engineering at Stanford University and developed microsystems integrated with heaters, temperature sensors, pressure sensors, and microchannel with distributed liquid injection to visualize and investigate two-phase transport phenomena in the microchannel for fuel cell applications. He is interested in exploring and teaching advanced science and technology in an inspiring way.

David Fogg received his B.S. degree (2000) from the Rensselaer Polytechnic Institute and his M.S. degree (2002) from Stanford University, all in mechanical engineering. He has spent two years in industry with Boeing and Knolls Atomic Power Lab. He is currently a Navy Nuclear Propulsion Fellow sponsored by the DOE and a doctoral candidate in Professor Goodson's group, working toward understanding transient phenomena in two-phase microchannel heat exchangers for the thermal management of microprocessors.

Roger Flynn is a Ph.D. student in Prof. Kenneth Goodson's Microscale Heat Transfer Laboratory at Stanford University. He received his B.S. in mechanical engineering from Washington State University (2002), and his M.S. in mechanical engineering from Stanford University (2003) before beginning his current research into boiling phenomena in microchannels. He is specifically involved with the design, characterization, and modeling of a parallel channel boiling flow heat exchanger for high heat flux cooling, but has interest in a variety of microscale heat transfer and fluid flow problems.

Eon Soo Lee received his B.S. degree in mechanical engineering at Yonsei University, Seoul, Korea, in 1999. Thereafter, he worked at Hyundai Heavy Industries. Since 2002, he has been part of the mechanical engineering department at Stanford University and received his M.S. degree in 2004. He is now pursuing a Ph.D. to understand the physics of two-phase flow and transport in microchannels with porous media, especially on the applications to Proton Exchange Membrane (PEM) fuel cells. His research interests are in the fluid mechanics and heat transfer of two-phase flow in microchannels and fuel cell energy systems.

Ching-Hsiang Cheng received his B.S. in mechanical engineering from National Taiwan University in 1993 and dual M.S. degrees in both mechanical and electrical engineering from Cornell University in 1998. In the same year, he joined Professor Khuri-Yakub's Ultrasonics Group in electrical engineering at Stanford University and received his Ph.D. degree in 2004. Following that, he joined Professor Goodson's Micro Heat Transfer Group in mechanical engineering at Stanford University as a post-doctoral scholar. His research interests include microfluidic cooling of electronics, water management of fuel cells, electrical through-wafer interconnects (ETWI), and capacitive ultrasonic transducers (CMUT).

Thomas W. Kenny received his B.S. degree in physics from the University of Minnesota, Minneapolis, in 1983 and his M.S. and Ph.D. degrees in physics from UC Berkeley, in 1987 and 1989, respectively. From 1989 to 1993, he worked at NASA JPL, where his research focused on the development of electron-tunneling high-resolution microsensors. In 1994, he joined the mechanical engineering department at Stanford University and directs MEMS-based research in a variety of areas, including resonators, wafer-scale packaging, cantilever beam force sensors, microfluidics, and novel fabrication techniques. He is a founder and CTO of Cooligy, a microfluidics chip cooling components manufacturer, and founder and board member of SiTime, a developer of CMOS timing references using MEMS resonators. Professor Kenny has authored and co-authored over 200 scientific papers and holds forty patents.

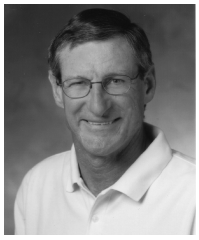

John K. Eaton is professor and vice-chairman of the mechanical engineering department at Stanford University, where he has been on the faculty since 1980. He is also the director of the GE/Stanford University Strategic Alliance. He conducts research in turbulence, particle-laden flows, convective heat transfer, and microscale multiphase heat transfer. He has supervised 38 completed Ph.D. dissertations, including those of twelve professors. He has won both the Tau Beta Pi and Perin Awards for teaching excellence, was an NSF Presidential Young Investigator Awardee, and is a fellow of the ASME.

Ken Goodson is an associate professor with the mechanical engineering department at Stanford University. After receiving the Ph.D. in mechanical engineering from MIT in 1993, Goodson worked with the Materials Research Group at Daimler-Benz AG on the thermal design of power circuits. In 1994, he joined Stanford, where his research group now includes twenty students and research associates. He has authored more than 120 journal and conference papers and five book chapters, and has been recognized through the ONR Young Investigator Award and the NSF CAREER Award as well as Best Paper Awards at SEMI-THERM (2001), the Multilevel Interconnect Symposium (1998), and SRC TECHCON (1998). He is a founder and former CTO of Cooligy, a Silicon Valley startup with 35 employees working on electroosmotic microchannel cooling systems for integrated circuits.